Emergence and suppressive function of Tr1 cells in glomerulonephritis

Shiwa Soukou-Wargalla*[1,2] and Christoph Kilian*[1,2], Lis Velasquez[1,2], Andres Machicote[1,2], Franziska Bertram[1,2], Friederike Stumme[1,2], Tanja Bedke[1,2], Anastasios Giannou[1,2,3], Jan Kempski[1,2], Morsal Sabihi[1,2], Ning Song[2,4], Hans-Joachim Paust[2,4], Alina Borchers[2,4], Laura Garcia Perez[1], Penelope Pelczar[1,2], Beibei Liu[1,2], Can Ergen[1,2], Babett Steglich[1,2], Franziska Muscate[2,3], Tobias B. Huber[4], Ulf Panzer[3,4], Nicola Gagliani[1,2,3], Christian F. Krebs[2,4,#] and Samuel Huber[1,2,#]

[1] I. Department of Medicine, University Medical Center Hamburg-Eppendorf, Hamburg, Hamburg, Germany

[2] Hamburg Center for Translational Immunology (HCTI), University Medical Center Hamburg-Eppendorf, Hamburg, Germany

[3] Department for General, Visceral and Thoracic Surgery, University Medical Center Hamburg-Eppendorf, Hamburg, Germany

[4] III. Department of Medicine, University Medical Center Hamburg-Eppendorf, Hamburg, Germany

* equally contributing first authors

[#] equally contributing senior authors

Correspondence to shuber@uke.de or c.krebs@uke.de

Summary

T regulatory type 1 (Tr1) cells, which are defined by their regulatory function, lack of Foxp3, high expression of IL-10, CD49b and LAG3, are known to be able to suppress Th1 and Th17 in the intestine. Th1 and Th17 cells are among the main drivers of crescentic glomerulonephritis, the most severe form of renal autoimmune disease. However, whether Tr1 cells emerge in renal inflammation or more importantly, whether they exhibit regulatory function during glomerulonephritis is unknown. In order to address these questions, we used a mouse model of experimental crescentic glomerulonephritis and double Foxp3^{mRFP} IL-10^{eGFP} reporter mice. We found that Foxp3^{neg} IL-10-producing CD4^{+} T cells infiltrate the kidneys during glomerulonephritis progression. Using single cell RNA-sequencing, we could show that these cells express the core transcriptional factors characteristic of Tr1 cells. In line with this, Tr1 cells showed a strong suppressive activity *ex vivo*, and were protective in experimental crescentic glomerulonephritis *in vivo*. Finally, we could also identify Tr1 cells in the human kidney of a patient with anti-neutrophil cytoplasmic autoantibody (ANCA)-associated glomerulonephritis, and were able to describe their transcriptional profile. Tr1 cells are currently used in several immune-mediated inflammatory diseases, such as T-cell therapy. Thus, our study sets the premise for Tr1 cell-based therapies in patients with glomerulonephritis.

Introduction

Immune-mediated inflammatory diseases (IMIDs) are characterized by an expansion of pro-inflammatory $CD4^+$ T-cell subsets, such as Th1 and Th17 cells. Accordingly, inflammatory diseases in the kidney, such as anti-neutrophil cytoplasmatic antibody (ANCA)-associated glomerulonephritis (GN), lupus nephritis and anti-glomerular basement membrane (anti-GBM) glomerulonephritis are characterized by an increase of effector $CD4^+$ T cells, especially of Th1 and Th17 cells [1-5]. Thus, one key aim is to understand how these cells can be therapeutically controlled. The immune system has several mechanisms by which effector $CD4^+$ T cells can be controlled in order to maintain and reestablish homeostasis. A first mechanism for controlling effector $CD4^+$ T cells is modulation via regulatory T cells. Foxp3 positive regulatory T cells ($Foxp3^{pos}$ Treg) are one anti-inflammatory T cells subset, which has been extensively studied in the context of GN [6-8]. It has been shown that $Foxp3^{pos}$ Treg, via the production of IL-10, can control Th17 cells in the kidney and the intestine [6, 9-11]. There is another anti-inflammatory T-cell subset, which is also known to produce high amounts of IL-10, namely regulatory type 1 T cells, otherwise referred to as Tr1 cells. Tr1 cells are $CD4^+$ T cells that are defined by the absence of Foxp3, expression of IL-10 and regulatory function [12, 13]. Interestingly, the suppressive activity of Tr1 cells also depends on functional IL-10 receptor signaling [9, 14, 15]. In fact, when Tr1 cells cannot respond to IL-10, they lose the capacity to maintain their own IL-10 production. Consequently, their suppressive activity declines [14]. Mouse Tr1-cell differentiation can be induced *in vitro* by the addition of the cytokine IL-27 [16]. Tr1 cells are identified via a combination of criteria: high IL-10 expression, lack of Foxp3, co-expression of the integrin alpha2 subunit (CD49b) and the lymphocyte-activation gene 3 (LAG-3) [13, 17]. Additionally, there are more co-inhibitory receptors which are known to be expressed by Tr1 cells, such as T cell immunoglobulin and ITIM domain (TIGIT), the transmembrane protein TIM-3 (TIM3), programmed cell death protein 1 (PD-1) and CCR5 that can help to identify Tr1 cells [6, 18]. Despite these data, it was unknown whether Tr1 cells are present in the kidney and whether they could potentially play a regulatory role in GN.

A second control mechanism relies on the potential of Th17 cells to change their phenotype and to acquire regulatory properties [19]. Indeed, Th17 cells can convert into regulatory T cells, referred to as $Tr1^{exTh17}$ cells [19]. In line with this, it had been shown that CD3-specific antibody treatment, which

is known to induce Tr1^{exTh17} cells in the intestine, is also able to induced IL-10 production in Th17 in the kidney and thus is protective in nephritic mice [1, 20]. However, despite this study, the emergence and function of Tr1 cells in glomerulonephritis remain unknown.

Therefore, we aimed here to study the emergence and function of Tr1 cells in the context of glomerulonephritis. By doing so, we found that Tr1 cells emerge in the kidney, but only a small fraction of these cells derived from Th17 cells. Moreover, functional *in vitro* as well as *in vivo* analysis confirmed that Tr1 cells have regulatory activity in the kidney in mouse models. Finally, we showed the existence of Tr1 cells in human kidney biopsies. Thus, this study forms the basis for targeting Tr1 cells in patients with glomerulonephritis.

Material & Methods

Animals

Mice were kept under specific pathogen free conditions in the animal research facility of the University Medical Center Hamburg-Eppendorf (UKE). Food and water were provided *ad libitum*. *Rag1*$^{-/-}$ were obtained from the Jackson Laboratory. *Il17a*^{Cre} *Il10Rα*$^{flox\ flox}$, *Il17a*^{Cre} *Il10*$^{flox\ flox}$ transgenic mice, *Foxp3*^{mRFP}, *Il17a*^{eGFP}, *Il17a*^{FP635}, *Il10*^{eGFP} reporter mice and *Il17a*^{Cre}, *Rosa26*^{YFP} are described elsewhere [13, 15, 21-23]. Age and sex matched littermates between 8-12 weeks were used. All animals were cared for in accordance to the institutional review board 'Behörde für Soziales, Familie, Gesundheit und Verbraucherschutz' (Hamburg, Germany) listed under the animal protocol number 17/2012.

Induction of experimental crescentic glomerulonephritis and functional studies

For the induction of the experimental crescentic glomerulonephritis (nephrotoxic nephritis, NTN), mice were injected intraperitoneally with anti-serum raised against the glomerular basement membrane [1]. For the measurement of albumin and creatinine levels, urine was collected at day 9 after disease induction. Urine samples were tested for creatinine concentration using the Creatinine Jaffé Fluid (Hengler Analytik, Steinbach, Germany). Albumin-levels were detected via standard ELISA analysis (Mice-Albumin Kit; Bethyl Laboratories, Montgomery, TX) and measured at 650 nm using an ELISA-reader.

Blood was taken at the day of examination and blood serum was analyzed for the concentration of urea nitrogen using a cobas analyzer (Roche, Basel, Switzerland).

Anti-CD3 specific antibody mouse model

Mice were injected intraperitoneally with 15 µg anti-CD3 specific antibody (Clone 2C11) dissolved in 100 µl PBS. Injections were performed on day 8 and 10 after induction of glomerulonephritis. Mice were sacrificed four hours after the second injection was applied.

T cell-differentiation and in vivo transfer model

Firstly, isolated spleens and lymph nodes were smashed through 100 µm cell strainer. Total cells were pelleted. For the transfer of $CD4^+$ T cells, first $CD4^+$ T cells were isolated via positive selection using Magnetic activated cell sorting (MACS) (Miltenyi Biotec, Bergisch Gladbach, Germany). APCs were isolated using the same method via CD4, CD3 negative selection. To avoid proliferation during *in vitro* culture, APCs were irradiated with 30 Gy.

For Th17 cell-proliferation, plates were coated with PBS containing 2 µg/ml anti-CD3 specific antibody. Plates were incubated overnight at 4°C or for 3 hours at 37°C. $1x10^6$ naïve $CD4^+$ T cells/ml isolated from reporter mice were cultured in full Click's medium that was supplemented with 10 % FBS, 1 % l- glutamine, 1 % penicillin/streptomycin and 1:1000 β- Mercaptoethanol. $4x10^6$ irradiated APCs/ml, anti-CD3 specific antibody (3 µg/ml) anti-CD28 (2 µg/ml) and TGF-β (0,5 ng/ml), IL-6 (10 ng/ml), IL-23 (20 ng/ml), anti-IFN-γ (10 µg/ml) and anti-IL-4 (10 µg/ml) was added to the full Click's medium. Cells were cultured for 5 days at 37°C – 5 % CO_2.

For Tr1-cell proliferation, 24 well plates were coated with PBS containing 2 µg/ml anti-CD3 specific antibody. Plates incubated overnight at 4°C or for 3 hours at 37°C. Prior culture, coating solution was removed completely. After depletion of $CD25^+$ cells, $1x10^6$ $CD4^+$ T cells/ml from reporter mice were resuspended in full Click's medium that contained anti-CD28 (2 µg/ml) and IL-27 (30 ng/ml). Cells were cultured for 5 days at 37°C 5 % CO_2. The expression of $Foxp3^{mRFP}$ and IL-10^{eGFP} was determined using flow cytometry.

Fluorescence-activated cell sorting (FACS-sorting) was performed on a BD FACS Aria Illu or AriaFusion. Th17 cells were FACS-sorted by negative expression of Foxp3mRFP and positive expression for IL-17AeGFP. $Foxp3^{neg}$ Tr1 cells were sorted for high expression of IL-10eGFP. $Foxp3^{pos}$ Tregs cells were isolated from spleens of reporter mice and sorted according to Foxp3mRFP expression. For the *in vivo* transfer, $1x10^5$ Th17 cells were either transferred alone or in combination with $2.5x10^3$ $Foxp3^{pos}$ Treg cells or $5x10^5$ Tr1 cells into *Rag1*$^{-/-}$ mice. This transfer was performed 24 hours prior the induction of crescentic glomerulonephritis.

Morphological examination

Light microscopy was performed on paraffin embedded, 1 µm thick, 4 % PFA fixed kidney cross sections stained with PAS-staining. The formation of crescents was assessed in 30 glomeruli per mouse in a blind manner.

Isolation of lymphocytes from different organs

Spleens and lymph nodes were smashed through 100 µm cell strainer and washed with PBS/1 % FBS followed by centrifugation. Spleens were further processed for erythrocyte lysis using Ammonium-Chloride-Potassium- (ACK) buffer.

Kidneys were crushed and incubated at 37 °C for 45 minutes in RPMI medium, containing 10 % FBS, 200 µg/ml DNAse I and 2 mg/ml Collagenase D. After incubation, the tissue was mechanically reduced to a pulp and cells were pelleted. A 37 % Percoll gradient centrifugation was performed. Remaining erythrocytes were lysed via ACK buffer.

For the isolation of intraepithelial lymphocytes (IELs), 0.5 cm pieces of the small intestines were incubated in 10 ml RPMI medium containing 10 % FBS and 1.5 mg DTT for 20 minutes at 37°C. For the isolation of lamina propria lymphocytes (LPLs), digested tissue was cut to a pulp and transferred in 6 ml Collagenase solution, RPMI medium containing 10 % FBS, collagenase (100 U/ml) and DNAse I (1000 U/ml) for 45 minutes at 37°C. LPLs were pelleted and pooled with IELs. For further cell separation, a 40 %/ 67 % Percoll gradient was performed (GE Healthcare). The leukocyte-enriched interphase was isolated, washed and processed for further staining steps.

Flow cytometry

In case of reporter mice, cells were analyzed after surface staining. To enable intracellular staining, in case of non-reporter mice, cells were stimulated for 3 hours at 37°C with PMA (50ng/ml; Merck Darmstadt), Ionomycin (1 mM; Sigma Aldrich).

To discriminate dead from living cells, isolated cells were pelleted and stained with a fluorochrome labeled violet DNA dye. Pacific OrangeTM Succinimidyl Ester (Life technologies, Lot 2179293) was diluted (1:1000) in PBS and incubated for 30 minutes at 4°C. Cells were washed and pelleted.

Surface staining panel for FACS analysis: CD11b (PE-Cy7, BioLegend, clone M1/70, Lot B249268, Dilution 1:400); CD11c (PE-Cy7, BioLegend, clone N418, Lot B222652, Dilution 1:400); CD195 (CCR5) (PE/Cy7, BioLegend, clone HM-CCR5, Lot B224462, Dilution 1:400); CD25 (BV650, BioLegend, clone PC61, Lot B288551, Dilution 1:100); CD3 (BUV379, BD, clone 17A2, Lot 9080908, Dilution 1:200); CD4 (Pac Blue, BioLegend, clone RM4-5, Lot B336509, Dilution 1:600; BV650, BioLegend, clone RM4-5, Lot B297638, Dilution 1:400); CD45 (BV785, BioLegend, clone 30-F11, Lot B336128, Dilution 1:800); CD45.1 (APC, BioLegend, clone A20, Lot B209251, Dilution 1:400); CD45.2 (PE Cy7, BioLegend, clone 104, Lot B307583, Dilution 1:400); CD8α (PE-Cy7, BioLegend, clone 53-6,7, Lot B295389, Dilution 1:400; NK1.1 (PE-Cy7, BioLegend, clone PK136, Lot B284829, Dilution 1:400); CD279 PD1 (BV 605, BioLegend, clone 29F.1A12, Lot B227579, Dilution 1:400); TCR-γδ (PE-Cy7, BioLegend, clone GL3, Lot B222125, Dilution 1:400); TIGIT (PerCPCy5.5, eBioscience, clone GIGD7, Lot 1988570, Dilution 1:400); CD366 (TIM-3) (BV 421, BioLegend, clone RMT3-23, Lot B259713, Dilution 1:400). Surface staining was performed for 20 minutes at 4°C.

CD49b (PE, BioLegend, clone HMa2, Lot B230820, Dilution 1:100); CD223 (LAG3) (APC, BioLegend, clone C9B7W, Lot B243438, Dilution 1:100) CD49b and LAG3 staining was performed for 30 minutes at 37°C.

In order to stain for intracellular markers, cells were fixed for 20 minutes with 4 % formaldehyde, followed by permeabilization of the cell membranes adding 0.1 % Nonidet P40 (NP40)- solution (Sigma Aldrich) for 4 minutes. Lastly, a staining cocktail with fluorochrome labeled antibodies for intracellular staining was added to the cells.

Foxp3 (APC, eBioscience, clone FJK-16s, Lot 2297415, Dilution 1:80; PE, eBioscience, clone NRRF-30, Lot 1927456, Dilution 1:80); IFN-γ (BV785, BioLegend, clone XMG1.2, Lot B343101, Dilution 1:100; APC, Biolegend, clone XMG1.2, Lot B288855, Dilution 1:100); IL-10 (PE-Dazzle, BioLegend, clone JES5-16E3, Lot B265048, Dilution 1:100); IL-17A (BV 421, Biolegend, clone TC11-18H10.1, Lot B318238, Dilution 1:100). Intracellular staining was performed for one hour at room temperature.

Fluorochrome detection was performed on an LSR II flow cytometer using FACS Diva software. For analysis, data were exported from the FACS Diva to FlowJo vX software for MAC or Windows.

In vitro suppression assay

Using MACS beads, responder cells ($CD4^+$, $CD25^-$) were isolated from spleen and lymph nodes and labeled with 5 µM violet dye. Per well $1.5x10^4$ responder cells together with $7.5x10^4$ APCs were plated in a 96-well round bottom plate. Next, $1x10^4$ Treg cells/well were added to the responder-APC-mix. Additional soluble anti-CD3 specific antibody (1.5 mg/ml final volume/well) led to further cell stimulation. After 96 hours at 37°C in a 5 % CO_2 incubator, the proliferation of responder cells was determined via FACS by detecting the intensity of violet dye per cell.

RNA isolation from sorted kidney cells to perform 10X single cell sequencing

After sorting of $6x10^4$ $Foxp3^{pos}$ IL-10-producing $CD4^+$ T cells from nephritic kidneys, the sample was processed with Chromium TM Single Cell 3' v2 kit according to the corresponding protocol of 10X Genomics™. The libraries were sequenced on an Illumina NovaSeq 6000 system (S4 flow cell) with 150 base pairs and paired- end configurations.

Data analysis of single cell sequencing

The mouse single cell RNA sequencing data was processed using CellRanger version 4.0.0. Further processing and downstream analysis of the single cell data was done using the R software version 4.1.1 (2021-08-10). We set the global seed to 0. If not mentioned otherwise, we ran the methods with default parameters. The R-Package Seurat (version 4.1.0) was used for pre-processing, dimensional reduction and cluster identification.

As part of quality check, we only kept cells that had at least >450 <4000 (control), >700 <4000 (anti-CD3) genes and a percentage of mitochondrial genes <35 %. Values were determined after visually inspecting the distribution. The two mouse datasets (control and anti-CD3) were integrated and scaled with regression of library size and percentage of mitochondrial gene and sex associated batches (regression of the added gene-expression of Xist + Tsix). Next, principal components (PC) were computed according to Seurat's pipeline. After Louvain clustering (PC 1 to 25, resolution 0.4) and UMAP visualizing (PC 1 to 25) we removed two clusters containing non-T-cells (like macrophages) as well as one cluster expressing primarily ribosomal genes, and another cluster expressing cell cycle genes. Finally, we gained 10,751 cells (control 3,139 cells, anti-CD3 7,612

cells). Next, we performed re-reclustering (resolution 0.4 and PC 1 to 25) and computed a new UMAP.

The preprocessed and clustered human data was received from [24]. The dataset was subset using only CD4 positive clusters, annotated with Th1, Th17, CD4_Tcm, Treg. Subsequently the patients were re-integrated (methods FindIntegrationAnchords (k.filter=50), IntegrateData(k.filter = 50) and cells were re-clustered (resolution 0.5, PC 1 to 30).

Scores were calculated using Seurat's method AddModulScore and the following mouse (or human equivalent) genes: Il10, Lag3, Havcr2, Pdcd1, Ctla4, Itga2, Tigit. Significance between datasets were determined using Wilcoxon rank sum test.

Statistical analysis

Statistical evaluations were performed using the GraphPad Prism software. Unpaired, nonparametric Mann-Whitney t-test or One-way ANOVA using Tukey's multiple comparisons-test were used for evaluation of statistical significance. A p-value < 0.05 was used to define significance.

Results

Analysis of IL-10-producing T cells in crescentic glomerulonephritis

The aim of this study was to investigate the emergence and function of Tr1 cells in the kidney. As IL-10 is the signature cytokine of these cells, we first analyzed the infiltration of the IL-10-producing $CD4^+$ T cells in the time course of crescentic glomerulonephritis (cGN). Fate+ reporter mice were used in order to enable simultaneous analyses of Foxp3, IL-10, and IL-17A expression simultaneously. Furthermore, as IL-$17A^+$ cells are permanently marked with YFP in this mouse, are also able to identify IL-10-producing cells that emerged from Th17 cells [19]. Experimental cGN was induced in Fate+ mice and we analyzed the kidneys over the course of the disease (Fig. 1a-c). As a control, we analyzed the frequency of these cells under steady state conditions (day 0). IL-10 expression was detected in $Foxp3^{pos}$ as well as in $Foxp3^{neg}$ $CD4^+$ T cells (Fig. 1d+e). Both IL-10-producing T-cell subsets were below 1% of CD4+ T cells in steady state, but frequencies increased with the onset of the disease at day 3 reaching the peak at day 7 - 10 (Fig. 1e). However, within $CD4^+$ T cells, the frequencies of $Foxp3^{neg}$ IL-10-producing $CD4^+$ T cells was about ten times higher compared to $Foxp3^{pos}$ IL-10-producing $CD4^+$ T cells (Figure 1e). We furthermore found that a small fraction (1 – 5%) of $Foxp3^{neg}$ IL-10-producing $CD4^+$ T cells were YFP positive, indicating that they are or have expressed IL-17A before (Fig. 1e).

Taken together, $Foxp3^{neg}$ IL-10-producing $CD4^+$ T cells emerge during the course of disease. Likewise, $Foxp3^{pos}$ IL-10-producing $CD4^+$ T cells increase but overall at about 10 times lower levels compared to $Foxp3^{neg}$ IL-10-producing $CD4^+$ T cells. Finally, about 5% of $Foxp3^{neg}$ IL-10-producing $CD4^+$ T cells originated from IL-17A-producing cells.

CD3 specific antibody treatment promotes IL-10-producing T cells in Glomerulonephritis

Next, we aimed to study whether we can further expand $Foxp3^{neg}$ IL-10-producing $CD4^+$ T cells in the kidney. To this end, we used anti-CD3 specific antibody treatment, which we have used before to suppress cGN [20] and which is known to induce IL-10 production in intestinal CD4+ T cells in the intestine [9, 17, 19, 23]. Again, experimental cGN was induced in Fate+ mice which were treated with antibodies against CD3 at days 8 and 10 post disease induction (Fig. 2a). $Foxp3^{neg}$ IL-10-producing $CD4^+$ T cells were further separated into Foxp3/ YFP double negative cells (IL-10-

producing cell, which did not emerge from Th17 cells), Foxp3 negative YFP positive IL-17A positive (IL-10-producing Th17 cells) and Foxp3 negative YFP positive IL-17A negative (IL-10-producing cells, which have produced IL-17A before (exTh17 cells)) (Fig. 2b). In line with previous data studying the intestine [9, 22] (Fig1. S1), CD3 antibody treatment strongly increased the frequency of IL-10 in all analyzed subsets in the kidney (Fig. 2c). Furthermore, we confirmed that some exTh17 cells expressed IL-10. Also, here the production of IL-10 was further promoted by CD3 antibody treatment (Fig. 2b+c).

A fraction of Foxp3^{neg} IL-10-producing CD4^{+} T cells in cGN expresses coinhibitory receptors

Next, we aimed to further characterize Foxp3^{neg} IL-10-producing CD4^{+} T cells in the kidney. We specifically analyzed the expression of CD49b and Lag3 as well as other co-inhibitory receptors (CIR), which are known to be expressed by Tr1 cells. We induced cGN in Foxp3^{RFP} IL-10^{eGFP} reporter mice. At day 8 and 10 days, half of the mice received an injection of antibodies against CD3. Control mice received PBS injections instead (Fig. 3a). In order to identify CIR-rich cells within Foxp3^{neg} IL-10-producing CD4^{+} T cells, we analyzed the co-expression of IL-10 and CD49b, Lag3, TIGIT and TIM3 via flow cytometry (Fig. S2a). We identified Foxp3^{neg} IL-10-producing CD4^{+} T cells that indeed additionally expressed CIR either alone or in combination with other markers (Fig. 3b+d). Of note, anti-CD3 antibody treatment also strongly induced the frequency of CIR (Fig. 3d+e).

Thus, anti-CD3 specific antibody treatment induced Foxp3^{neg} IL-10-producing CD4^{+} T cells, which do express CIR and thus are referred to as Tr1 cells.

Single cell sequencing reveals that a fraction of Foxp3^{neg} IL-10-producing CD4^{+} T cells in cGN expresses the core transcriptional program of Tr1 cells

On the basis of these data, we next aimed to use an unsupervised approach in order to confirm that the Foxp3^{neg} IL-10-producing CD4^{+} T cells in the kidney are indeed Tr1 cells, and therefore, do express the signature genes of this cell type. To this end, we used single cell sequencing. We induced experimental glomerulonephritis in Foxp3^{RFP} IL-10^{eGFP} reporter mice and treated half of them with antibodies against CD3 (Fig. 4a). The control group received PBS instead. Foxp3^{neg} IL-10-producing CD4^{+} T cells were FACS sorted and then subjected to single cells sequencing using 10X

genomics (Fig. 4a, S3a). After quality control, a total of 10,751 cells (control: 3,139 cells, anti-CD3: 7,612 cells) were analyzed. This analysis revealed a heterogeneous cell population that separated into seven distinct clusters (C1-C7) (Fig. 4b). While most of the clusters showed a gene signature towards effector like cells, we identified two cluster (C3, C4) being enriched with CIR (Fig. 4b, 4f). Moreover, we specifically focused on the identification of Tr1 cells, expanding the genes to identify them. In accordance to the enriched CIR expression, cluster C3 and C4 also present the highest Tr1 score (a combination of *Il10*, *Lag3*, *Havcr2*, *Pdcd1*, *Ctla4*, *Itga2*, *Tigit*) (Fig. 4d). Furthermore, when comparing the genes expression of CIR-enriched clusters (C3, C4) with the remaining clusters, multiple genes being associated with a Tr1 phenotype were among the top differential expressed (DE) genes (Fig. 4f). Noteworthy, especially cluster C3 contains a fraction of cells expressing typ II inflammatory response signature cytokines as *Il13* and *Il4*. As shown in figure 3 the treatment with anti-CD3 specific antibody increased the frequency of CIR expressing Foxp3^{neg} IL-10-producing CD4^{+} T cells. On this basis, we compared the relative distribution of cells from the control and anti-CD3 group in each cluster (Fig. 4c). Here, the additional treatment with antibodies against CD3 led to a relative shrink of clusters, expressing a Th-17-like phenotype (C6, C7), but a relative increase of clusters C3, C4 and C5 (Fig. 4c). Comparing all cells from the control and anti-CD3, the Tr1 score was significantly increased in cells derived from mice treated with anti-CD3 antibody (Fig. 4e).

Taken together, we identified Foxp3^{neg} IL-10-producing CD4^{+} T cells in murine nephritic kidneys, which express the core transcriptional program of Tr1 cells (clusters C3, C4). This fraction was further expanded upon anti-CD3 specific antibody treatment.

Kidney-derived IL-10 producers show suppressive activity *in vitro*

On the basis of the above-mentioned data, we next aimed to evaluate the suppressive capacity of kidney-derived Foxp3^{neg} IL-10-producing CD4^{+} T cells. To this end, we first used an *in vitro* assay. CD4^{+} CD25-depleted cells (responder cells) were isolated from the spleens of mice in steady state and stained with a proliferation dye. During cell division, the intensity of the dye is halved to both daughter cells [25]. To obtain IL-10-producing T cells, experimental cGN was induced in Foxp3^{RFP} IL-10^{eGFP} reporter mice, and Foxp3^{pos} CD4^{+} T cells as well as Foxp3^{neg} IL-10-producing CD4^{+} T cells were sorted out from the kidneys 10 days after disease induction and their suppressive function

assessed *in vitro* (Fig. 5a). As a negative control, regulatory T cells were exchanged with the same numbers of non-suppressive $CD4^+$ responder cells. The dye was measured after five days using flow cytometry (Fig. 5b). When the violet dye intensity was analyzed in the responder cells, the negative control did not show any suppression but rather enhanced proliferation of responder cells (Fig. 5b-c). Addition of kidney-derived $Foxp3^{neg}$ IL-10-producing $CD4^+$ T cells inhibited proliferation of almost 85 % of the responder cells (Fig. 5b-c), which was comparable to the one observed by $Foxp3^{pos}$ Tregs (Fig. 5b-c).

Taken together, *ex vivo* isolated Tr1 cells from the kidney could suppress the proliferation of $CD4^+$ responder T cells *in vitro* to a similar degree as $Foxp3^{pos}$ Treg.

***In vitro*-generated Tr1 cells suppress cGN**

Tr1 cells are known to be efficient regulators of $CD4^+$ T-cell driven inflammation in the intestine. Whether they could also be used to suppress cGN has never addressed before. Thus, we aimed to assess the function of $Foxp3^{neg}$ IL-10-producing $CD4^+$ T cells in the context of glomerulonephritis. Th17 cells have been shown to promote glomerulonephritis when transferred in *Rag1*$^{-/-}$ mice [1]. Thus, to assess the suppressive capacity of Tr1 cells to inhibit Th17 cell driven glomerulonephritis, co-transfer experiments were performed (Fig. 6a). Since a high cell number is required for this experiment, both Th17 and Tr1 cells were differentiated *in vitro* (Fig. 6b). $Foxp3^{pos}$ Treg cells isolated from the spleens of untreated mice in steady state were used as a positive control. Th17 cells were transferred into immune incompetent *Rag1*$^{-/-}$ mice alone or in combination with stated regulatory T cells (Fig. 6a+c). About 24 hours after, glomerulonephritis was induced in the mice and the survival rate was monitored over the course of disease (Fig.6c-d). Mice that received only Th17 cells showed increased mortality compared to mice that received additional regulatory cells (Fig. 6d). Also, the glomerular damage analyzed in kidney cross sections, revealed the highest score in mice that received Th17 cells alone (Fig. 6e-f). Both groups that received either Tr1 cells or $Foxp3^{pos}$ Tregs cells displayed not only increased survival but also less crescent formation (Fig. 6d-f).

In conclusion, *in vitro*-differentiated Tr1 cells were sufficient suppressors of Th17 cell-mediated glomerulonephritis *in vivo*.

Identification of Tr1 cells in ANCA patients a proof of concept

Finally, we aimed to translate these findings to human biology. To this end, as proof of concept, we took advantage of single cell data from kidney biopsies isolated from an ANCA-patient (Fig. 7a) [24]. UMAP analysis identified eight different clusters within human-derived $CD4^+$ T cells from kidney biopsies of ANCA patients (Fig. 7b). We specifically aimed for the identification of $Foxp3^{neg}$ $CD4^+$ T cells that express the cytokine IL-10 and are CIR-enriched as these cells might be Tr1 cells. For CIR-enrichment, we depicted cells with at least two co-expressed CIR (Fig. 7c). Through this approach, we identified cluster of cells that expressed at least two or more markers at the same time. Next, we identified cells that showed an increased Tr1 score (combination of *IL10, LAG3, HAVCR2, ITGA, PDCD1, TIGIT* (Fig. 7d). This score was elevated in the clusters C2 and C5 (Fig. 7d). By analyzing further expression levels of genes encoding for CIR, IL-10 and Treg associated genes as *FOXP3* and *IL2RA* we identified cluster C5 to be enriched for $Foxp3^{pos}$ Tregs cells (Fig. 7e). To this end, we were able to identify cluster C2, that showed low gene expression for *FOXP3* and *IL2RA*, as our cluster of interest named Tr1. These data indicate that Tr1 cells may also be present in the kidney in patients with ANCA nephritis.

Discussion

This study aimed to address the potential of Tr1 cells to be used as T cell-based therapy for crescentic glomerulonephritis (cGN). To this end, we analyzed the emergence of Tr1 cells, identified their molecular profile and tested their functionality in the context of experimental glomerulonephritis. We found that Tr1 cells emerge, albeit at low numbers, during experimental glomerulonephritis, and proved their high level of suppressive activity *in vitro*. Importantly, Tr1-cell transfer was protective in a mouse cGN model. Thus, our study sets the premise to therapeutically target Tr1 cells in cGN.

Foxp3^{pos} Treg cells have been described as being able to ameliorate kidney injury by suppressing Th17 cell-mediated pathology via IL-10 [8]. Their power to stabilize immune homeostasis was found to be common for different organs and diseases, e.g. kidney and intestine [6, 9]. In the intestine, besides Foxp3^{pos} Treg cells, Tr1 cells can also suppress Th17 cell-driven colitis [9, 26]. However, whether Tr1 cells are also present in the kidney has not yet been addressed. Of note, Tr1 cells are defined by the expression of IL-10 and co-inhibitory receptors as well as by their regulatory function. Thus, we first studied the emergence of IL-10-producing CD4^{+} T cells in the kidney. Even under steady state conditions, we could detect some IL-10-producing CD4^{+} T cells in the kidney. Indeed, as the disease progressed, frequencies of IL-10 strongly increased in both Foxp3^{pos} and Foxp3^{neg} CD4^{+} T cells. Of note, in the disease setting, the number of Foxp3^{neg} IL-10-producing CD4^{+} T cells in the kidney was about ten times higher than the number of Foxp3^{pos} IL-10-producing Tregs. These data indicating that Tr1 cells may not only be present in the colon [27], but also in the kidney.

We next aimed to determine the origin of the Foxp3^{neg} IL-10-producing CD4^{+} T cells identified in the inflamed kidney. Of note, it had been shown before that Th17 cells can co-produce IL-10. Furthermore, in the intestine it was shown that Th17 cells can completely transdifferentiate into Tr1 cells (referred to as Tr1^{exTh17}), a process called T cell plasticity [19]. While Th17 cells in the brain of EAE mice have the capacity to convert into Th1 cells, Th17 cells in the kidney have been described to be more stable in terms of their cytokine expression and to not convert into Th1 cells to a large extent [20]. To investigate whether Th17 cells found in the kidneys of nephritic mice are able to convert to Tr1 cells, we used Fate+ fate mapping mice. We found that a fraction of Foxp3^{neg} IL-10-producing CD4^{+} T cells originated from Th17 cells. Thus, we demonstrated Th17 cell plasticity towards Tr1 cells. By tracking Th17 cells, we also identified cells co-producing IL-17 and IL-10.

However, the large majority of Foxp3^{neg} IL-10-producing CD4^{+} T cells did not originate from Th17 cell or co-produced IL-10 and IL-17.

To further characterize Foxp3^{neg} IL-10-producing CD4^{+} T cells, we performed multi-parameter flow cytometry analyzing the expression of co-inhibitory receptors and single cell sequencing of cells. To that end, we isolated cells from the kidney of mice with glomerulonephritis and nephritic mice that were additionally treated with CD3 specific antibodies as CD3-specific antibody treatment was shown before to induce expansion of Foxp3^{neg} IL-10-producing CD4^{+} T cells in the intestine [9, 19, 23]. This approach confirmed that a fraction of Foxp3^{neg} IL-10-producing CD4^{+} T cells from the kidney expressed co-inhibitory receptors and showed the transcriptional signature of a Tr1 cell in inflamed kidney. For both samples, the clustering of the total cells displayed a heterogeneous cell population. While some clusters revealed gene expression levels associated with effector cells, others displayed regulatory like gene expression pattern. This is in line with previous data showing that in the small intestine and the spleen there was a strong heterogeneity of IL-10-producing CD4^{+} T cells [17].

To build upon these descriptive data, we aimed to gain final confirmation regarding whether kidney-derived Foxp3^{neg} IL-10-producing CD4^{+} T cells would fulfil the ultimate criterion defining Tr1 cells, i.e. regulatory activity. We performed *in vitro*-suppression assays [28] with Foxp3^{neg} IL-10-producing CD4^{+} T cells from the kidneys of nephritic mice and proved that these cells indeed have a regulatory function *in vitro*. Thus, one could envision to use these cells as means of T cell-based therapy. However, in order to form the basis for this, one needs to further show their regulatory function *in vivo*. Indeed, during ongoing kidney inflammation, Foxp3^{pos} IL-10-producing Treg cells are present and increase in numbers during disease progression [29]. These cells have been shown to be able to suppress CD4^{+} T cell driven inflammation in the kidneys [8, 30, 31]. Thus, we wanted to go further and determine the suppressive capacity of Tr1 cells, in an *in vivo* Th17 cell transfer model for glomerulonephritis [1]. We performed an *in vivo* transfer experiment of Th17 cells alone or together with Tr1 cells and Treg cells respectively into *Rag1*$^{-/-}$ prior to induction of glomerulonephritis. To this end, regulatory T cells had to be first generated *in vitro* as it was not possible to obtain a sufficient number of Tr1 cells from the kidney for these experiments. Strikingly, our data indicate that *in vitro* differentiated Tr1 cells are capable of suppressing Th17 cell mediated glomerulonephritis. Thus, our data form the basis to establish a Tr1 based T-cell therapy for rapidly progressing glomerular

nephritis (RPGN), similar to what is already done in inflammatory bowel disease (IBD) patients [32, 33].

Finally, in order to further support this, we aimed to prove the existence of Tr1 cells in human kidneys. Therefore, we were especially interested in ANCA-patients. Thus, as proof of concept, we took advantage of unpublished single cell transcriptome data from one ANCA patient [24]. We focused on $CD4^+$ cells that expressed CIR and other surface markers. We shed light on the population of IL-10-producing $CD4^+$ T cells and finally, showed the pattern of a regulatory Tr1 cell in human diseased kidneys.

In conclusion, we identified Tr1 cells in mouse and human diseased kidney. These cells have a significant suppressive activity in a mouse model of cGN. Thus, our data form the basis not only to identify Tr1 cells in cGN-patients, but also to potentially develop personalized T cell therapies for patients with crescentic glomerulonephritis.

Acknowledgements

We thank the FACS Sorting Core Facility and the Single Cell Core Facility of the University Medical Center Hamburg-Eppendorf for their support. We thank Cathleen Haueis, Sandra Wende and Anett Peters for their excellent technical assistance. This work was supported by a grant from the *Deutsche Forschungsgemeinschaft* (DFG) (SFB1192 project A5 to C.F.K. and S.H.) and a grant of the *Forschungsförderungsfonds der Medizinischen Fakultät* (FFM) to S.S.-W..

Author information

These authors contributed equally:

Shiwa Soukou-Wargalla, Christoph Kilian

Christian F. Krebs, Samuel Huber

Authors and Affiliations

I. Department of Medicine, University Medical Center Hamburg-Eppendorf, 20246, Hamburg, Germany

Shiwa Soukou-Wargalla, Christoph Kilian, Lis Velasquez, Andres Machicote, Friederike Stumme, Franziska Bertram, Tanja Bedke, Jan Kempski, Morsal Sabihi, Penelope Pelczar, Beibei Liu, Can Ergen, Babett Steglich, Samuel Huber

III. Department of Medicine, University Medical Center Hamburg-Eppendorf, Hamburg, Germany

Christian F. Krebs, Hans-Joachim Paust, Ning Song, Ulf Panzer, Tobias B. Huber, Alina Borchers

Hamburg Center for Translational Immunology, University Medical Center Hamburg-Eppendorf, Hamburg, Germany

Tobias B. Huber, Ulf Panzer, Nicola Gagliani, Christian F. Krebs, Samuel Huber

Department for General, Visceral and Thoracic Surgery, University Medical Center Hamburg-Eppendorf, Hamburg, Germany

Anastasios Giannou, Nicola Gagliani, Franziska Muscate

OneChain Immunotherapeutics, University of Barcelona, Barcelona, Spain

Laura Garcia Perez

Ethics declarations

Competing interests: The authors declare no competing interests.

Main Figures

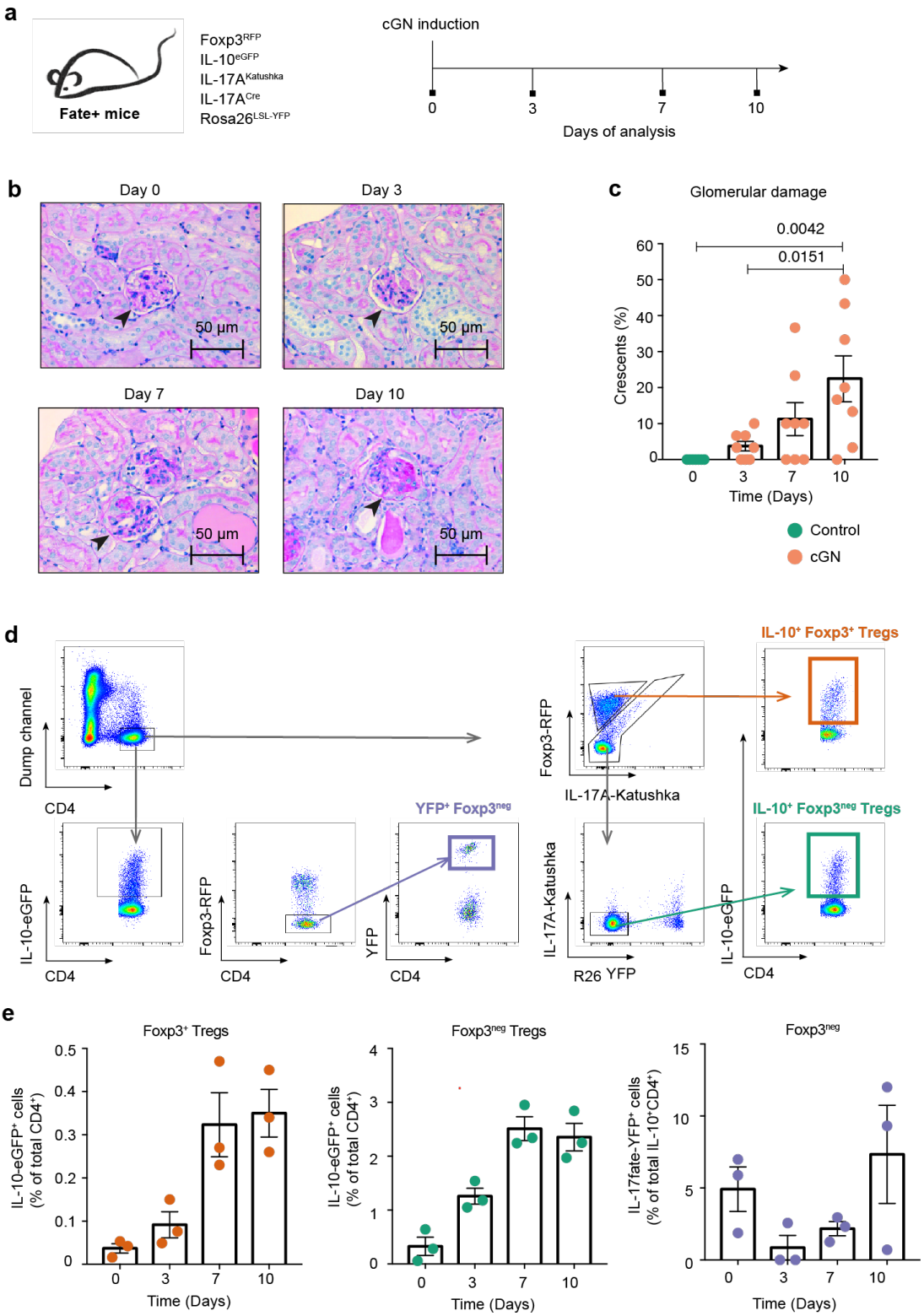

Figure 1: Emergence of IL-10-producing T cells in Glomerulonephritis

a) Experimental cGN was induced in *Foxp3^{mRFP} Il10^{eGFP} Il17a^{Katushka} Il17a^{Cre} Rosa26^{YFP}* (Fate+) mice. Animals were sacrificed under steady state conditions as well as day 3, 7 and 10 days after disease induction. Cells were isolated from kidneys. **b)** Representative PAS staining of Paraffin-embedded kidney cross sections **c)** Statistical analysis of percent (%) of crescents within 30 analyzed glomeruli. Data are representative of two independent experiments One-way ANOVA; Turkey's multiple comparisons test ($p<0.05$). Day 0 n=7, day 3 n=8, day 7 n=8, day 10 n=8. **d)** representative dot plots and gating strategy **e)** Scatter plots are shown (lines indicate mean ± SEM). Data are representative for of three independent experiments. Day 0 n=3, day 3 n=3, day 7 n=3, day 10 n=3.

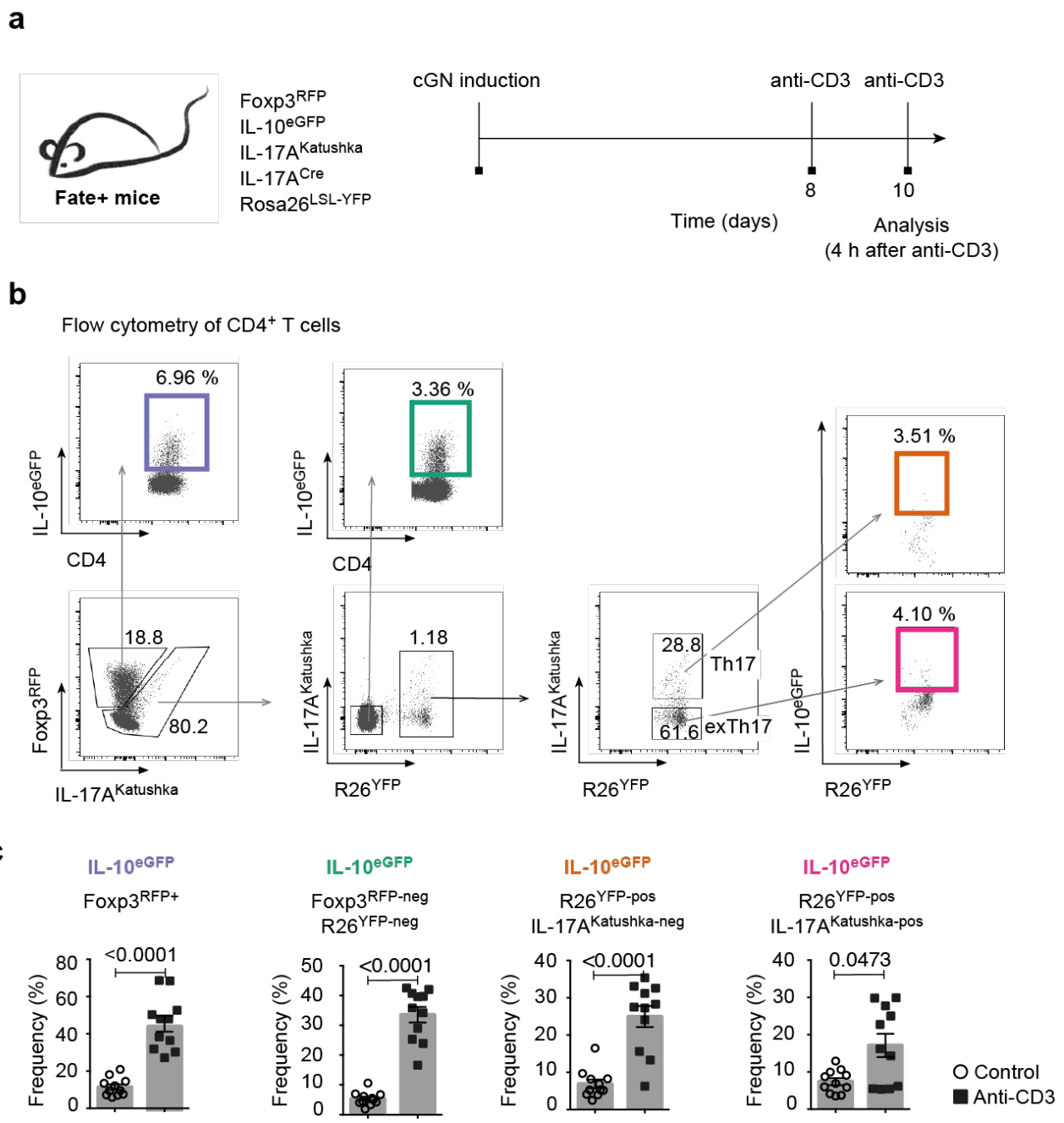

Figure 2: Expansion of IL-10-producing T cells in Glomerulonephritis upon CD3-specific antibody treatment

a) Experimental cGN was induced in *Foxp3*^{mRFP} *Il10*^{eGFP} *Il17a*^{Katushka} *Il17a*^{Cre} *Rosa26*^{YFP} (Fate+) mice separated in two groups. One group received additional 15 µg of anti-CD3 specific antibody on days 8 and 10 post disease induction. Control group received PBS instead. Mice were sacrificed 4 hours after the last antibody or PBS injection. Cells were isolated from kidneys. Frequencies (%) of Foxp3, IL-17A and IL-10 cells were measured by flow cytometry. **b)** Representative dot plots and gating strategy. **c)** Scatter plots are shown (lines indicate mean ± SEM). Kidney data are cumulative of four independent experiments. Mann Whitney test $p<0.05$. Control n=11 anti-CD3 n=11.

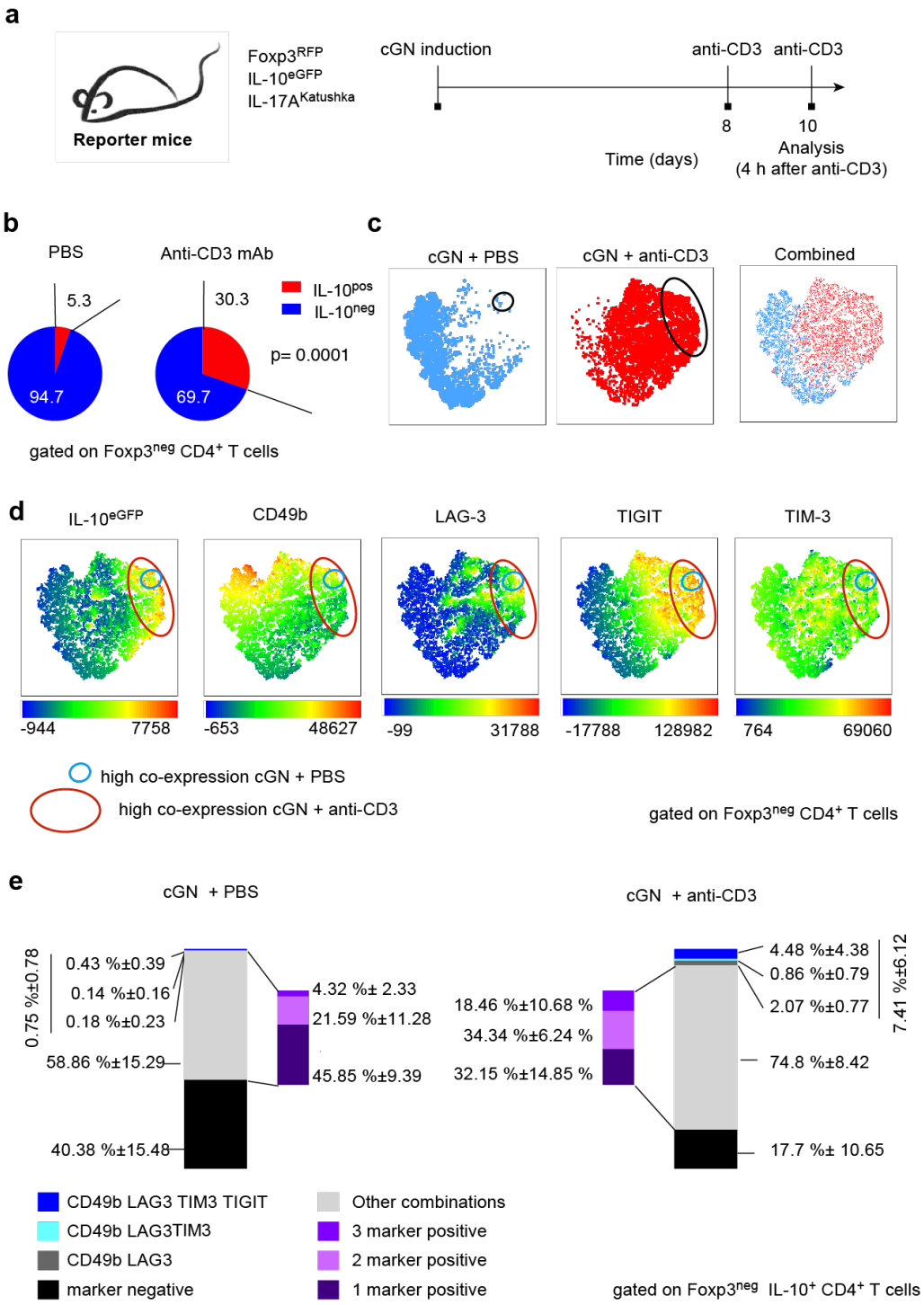

Figure 3: Identification of Tr1 cells within the IL-10-producing T cell subset on the basis of extra cellular markers

a) Glomerulonephritis was induced in Foxp3^{mRFP} IL-10^{eGFP} IL-17A^{Katushka} mice. Cells were isolated ten days after disease induction from the kidneys of nephritic mice. Analysis of IL-10 and co-stimulatory profile expression (CD49b, LAG-3, TIM-3, TIGIT) in Foxp3^{pos} CD4^{+} T cells after glomerulonephritis with and without anti-CD3 specific antibody treatment was performed. **b)** Pie chart shows expression of IL-10 gated on Foxp3^{pos} CD4^{+} T cells **c)** tSNE graphs shows cell distribution coming from alone control, anti-CD3 group or combined **d)** tSNE graphs shows expression of IL-10 or co-stimulatory surface markers gated on Foxp3^{pos} CD4^{+} T cells. **e)** Bar charts show distributions of stated marker combinations gated on Foxp3^{neg} IL-10-producing CD4^{+} T cells. Data are representative of three independent experiments. Mann Whitney test $p<0.05$. PBS n= 11, anti-CD3 n=6.

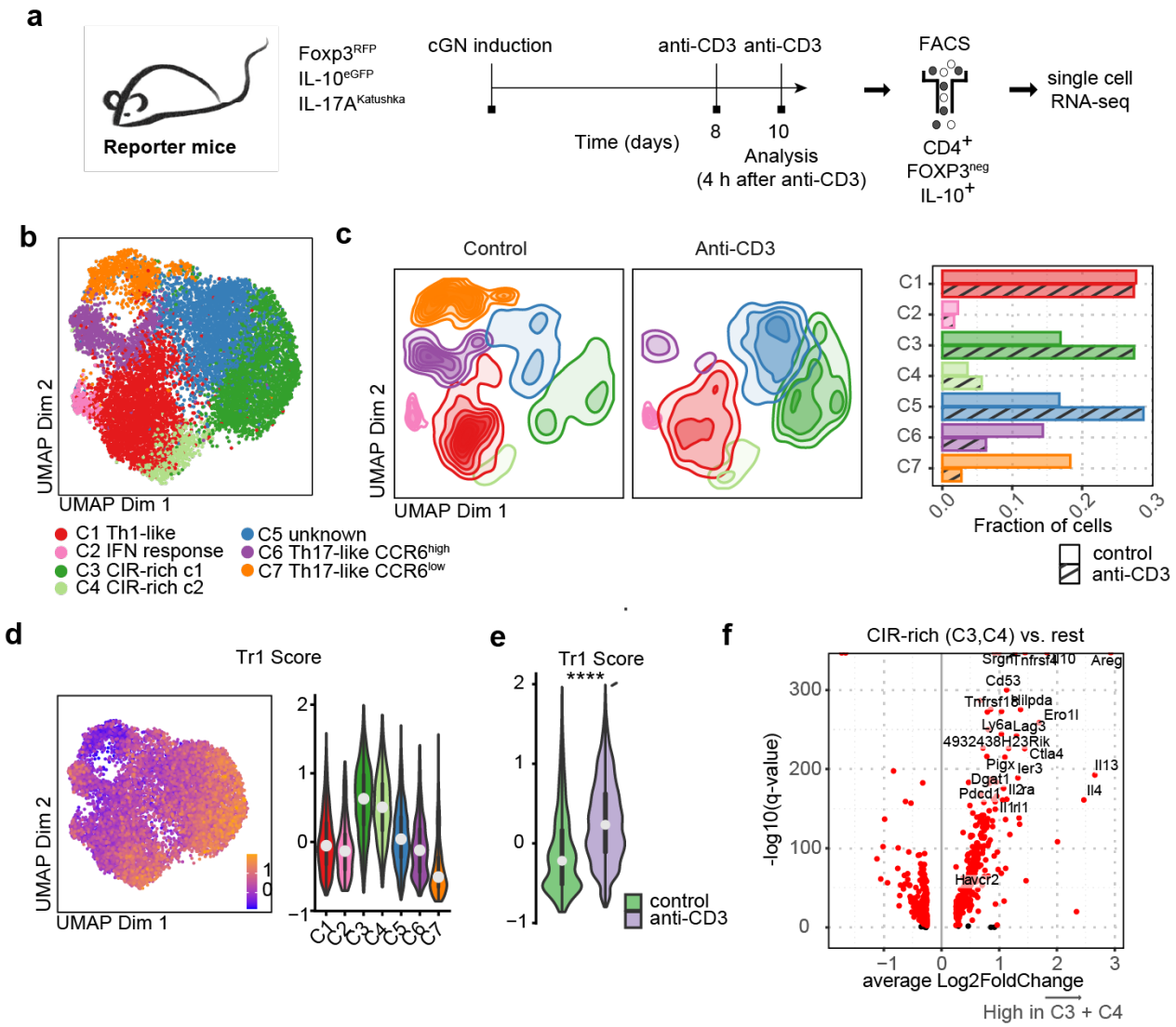

Figure 4: A subset of IL-10-producing T cells in the kidney expresses the core transcriptional program of Tr1 cells

a) Glomerulonephritis was induced in Foxp3^{mRFP} IL-10^{eGFP} IL-17A^{Katushka} mice. The experimental setup indicated that one group received additional 15 µg of anti-CD3 specific antibody on days 8 and 10 post disease induction. Control group received PBS instead. Mice were sacrificed 4 hours after the last antibody or PBS injection. Cells were isolated from the inflamed kidneys and Foxp3^{neg} IL-10-producing CD4^{+} T cells from the kidneys were sorted **b)** UMAP with colored cell clusters (C1 – C7). Identification of each cluster analyzed in a combined approach of CD4^{+} IL-10-producing cells from control group and anti-CD3 treated mice **c)** Spreading of sequenced T cells of mice treated with cGN serum alone (control) or in combination with antibodies against CD3 (anti-CD3) over the identified clusters, visualized as density-UMAP and barplot showing fraction of cells **d)** UMAP and Violin plot of Tr1-signature score in clusters C1-C7 in control group and anti-CD3 treated mice **e)** Violin plot comparing Tr1 score in control and anti-CD3 sample. (****) p-value < 0.0001. **f)** Volcano plot of differentially expressed genes comparing CIR-enriched clusters (C3, C4) versus the rest. Significant genes (FDR adjusted p-value < 0.01) colored red. Highly significant genes or significant CIR-genes are annotated in the plot.

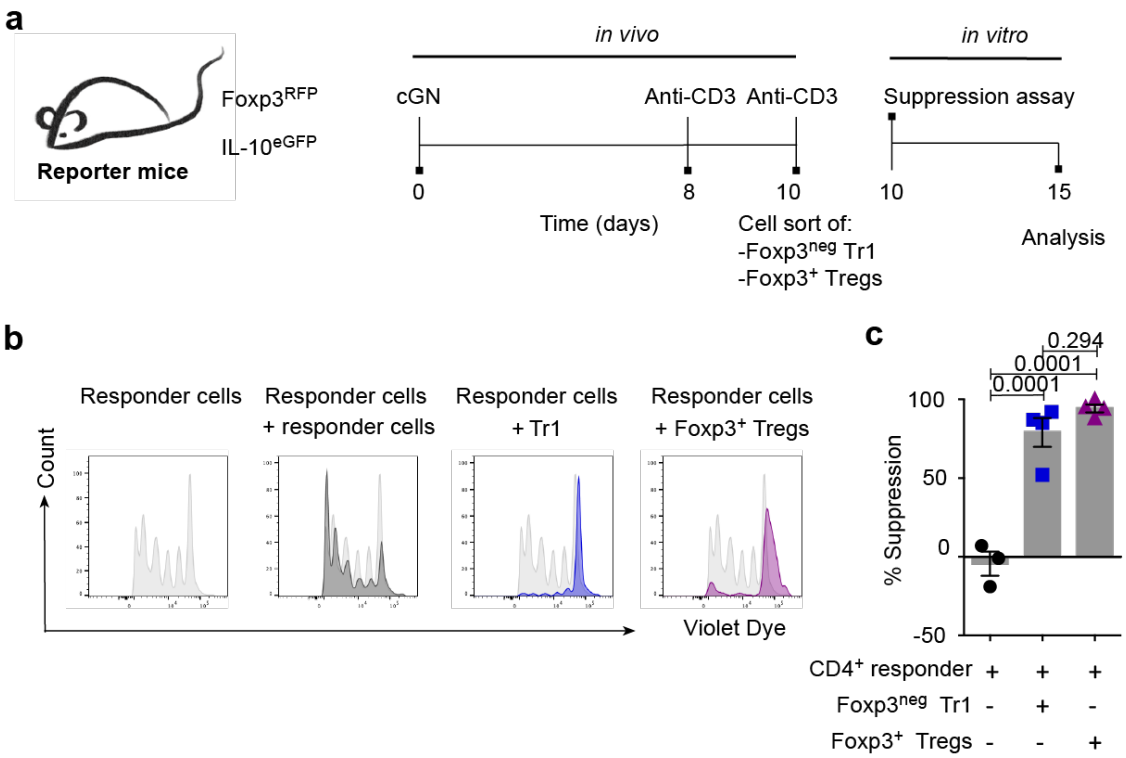

Figure 5: Tr1 cells from the kidney have *in vitro* suppressive activity

a) Glomerulonephritis was induced in Foxp3^{mRFP} IL-10^{eGFP} mice. Mice received additional 15 µg of anti-CD3 specific antibody on days 8 and 10 post disease induction. Mice were sacrificed 4 hours after the last antibody injection and suppressor cells were isolated from the inflamed kidneys. 1.5 x 10^4 CD4$^+$ T cells (responder cells) were plated per well. Additional 7.5 x 10^4 irradiated APCs served the purpose of cell activation. 1x10^4 suppressor cells were add to each well. Violet dye intensity was measured via flow cytometry **b)** Histograms and **c)** statistical analysis of violet dye intensity in CD4$^+$ responder cells after 5 days *in vitro* culture. Data are representative of three independent experiments. One-way ANOVA; Turkey's multiple comparisons test ($p<0.05$). Responder + responder n=3; responder + Foxp3$^-$ Tr1 n=4; responder + Foxp3$^+$ Tregs n=4.

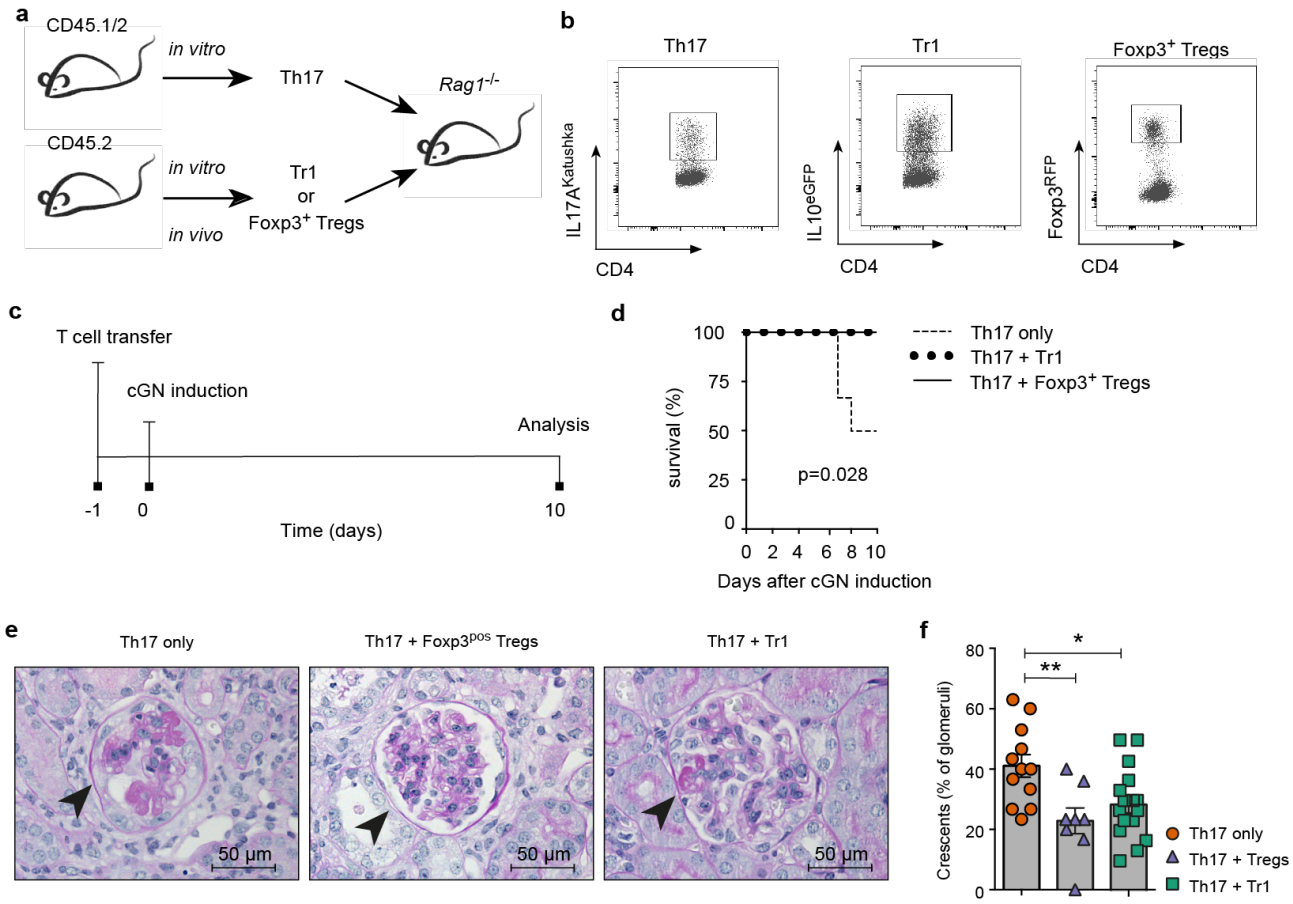

Figure 6: Tr1 cells suppress experimental glomerulonephritis *in vivo*

a+c) Th17 and Tr1 cells were differentiated *in vitro* from CD4$^+$ T cells. Foxp3$^+$ Tregs cells were isolated from spleens of steady state mice. **b)** Indicates representative dot plots and the gating strategy of stated T cell populations. c) Th17 cells were transferred into Rag1 knock out (Rag1$^{-/-}$) mice either alone or in combination with Tr1 cells or Foxp3$^+$ Treg cells as a control. Glomerulonephritis was induced to the mice 24 hours after cell transfer **d)** Survival data show overall survival of two independent experiments. Th17 only n=6 Th17 + Tr1 n=6 Th17 + Foxp3$^+$ Tregs n= 5. Statistics for survival curve: Comparison of survival curves; Log-rank (Mantel-Cox) test for trend $p<0.05$. **e)** Representative PAS staining of Paraffin-embedded kidney cross sections **f)** Statistical analysis of percent (%) of crescents within 30 analyzed glomeruli. Data are representative of five independent experiments. Th17 only n=12 Th17 + Tr1 n=17 Th17 + Foxp3$^+$ Tregs n= 8. Scatter plots are shown (lines indicate mean ± SEM) Statistic for crescents: One-way ANOVA; Turkey's multiple comparisons test ($p<0.05$).

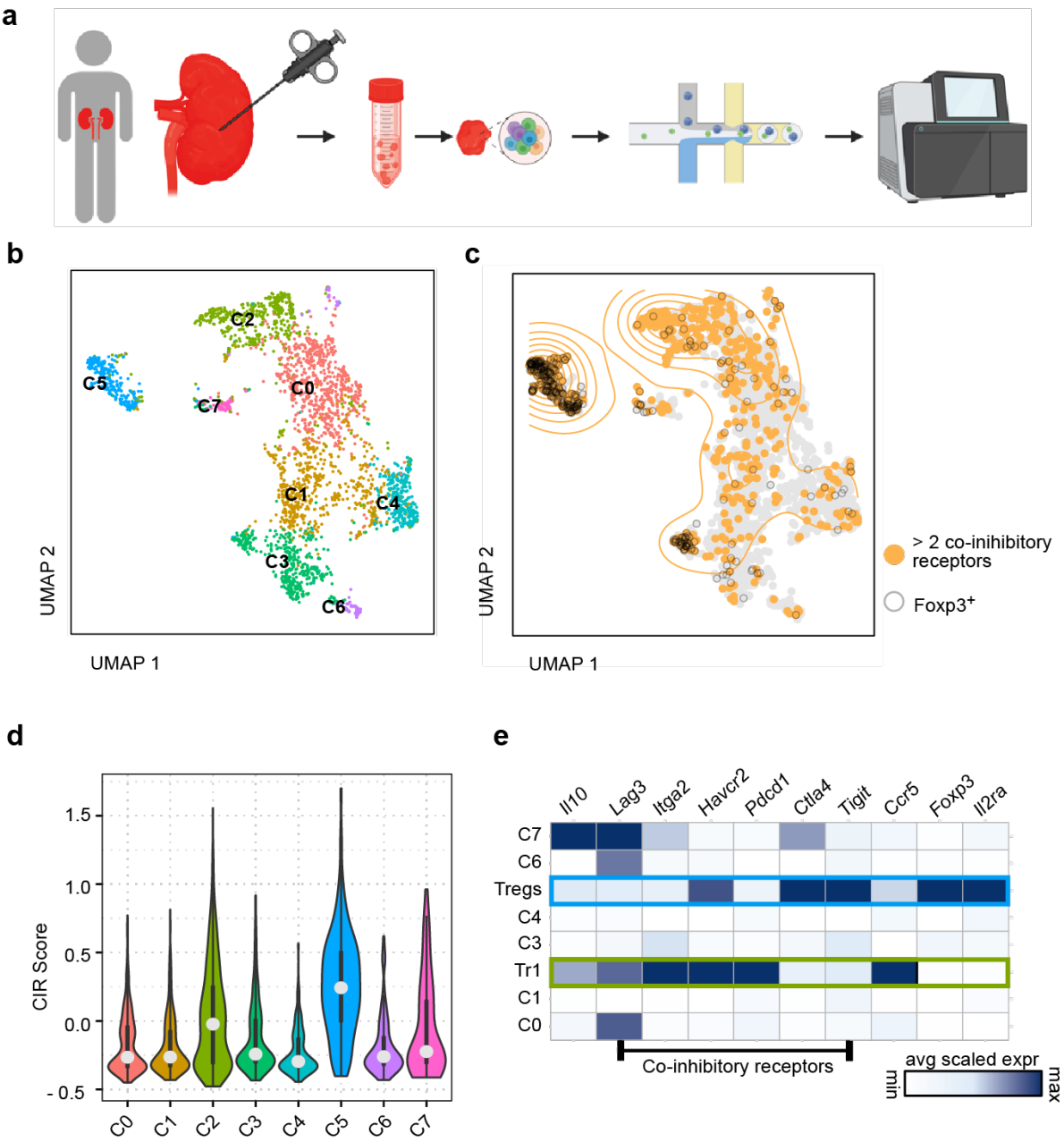

Figure 7: Identification of Tr1 cells in ANCA patients

a) Kidney biopsy was isolated from one ANCA Patient. Biopsy was reduced to a single cell suspension. Cells were barcoded and single cell sequencing was performed **b)** $CD4^+$ cells of the original dataset, visualized as UMAP with cells colored according to the clustering of $CD4^+$ T cells **c)** UMAP of single cells expressing Foxp3 (black circle) and at least two co-inhibitory receptors (orange color). Orange lines represent the density distribution of orange-colored cells. **d)** Violin-Plot of cluster C0-C7 of the Tr1/CIR score. **e)** Average expression per cluster of manually selected genes. Values were normalized for gene-wise across the clusters and colored according to the maximal and minimal value per gene.

Suppl. Figures

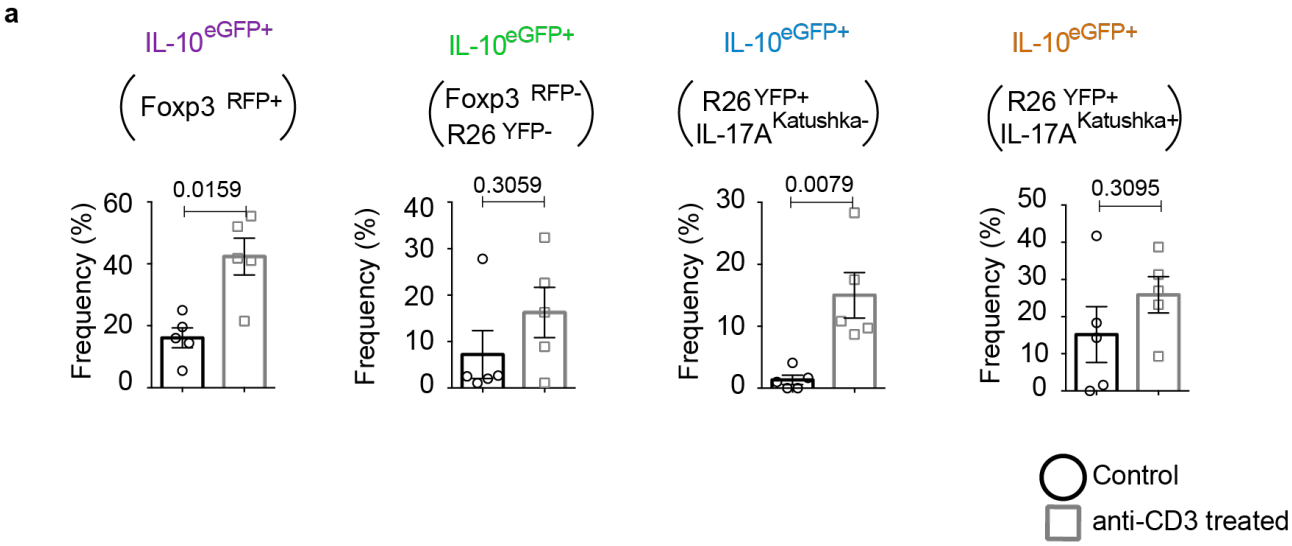

Figure S1: CD3-specific antibody treatment induces IL-10-producing T cells in the gut of nephritic mice

Experimental cGN was induced in *Foxp3*^{mRFP} *Il10*^{eGFP} *Il17a*^{Katushka} *Il17a*^{Cre} *Rosa26*^{YFP} (Fate+) mice separated in two groups. One group received additional 15 µg of anti-CD3 specific antibody on days 8 and 10 post disease induction. Mice were sacrificed 4 hours after the last antibody injection. Control group received PBS instead. Cells were isolated from the small intestine. a) Data are cumulative of three independent experiments. Control n=5 anti-CD3 n=5 Mann Whitney test $p<0.05$.

a

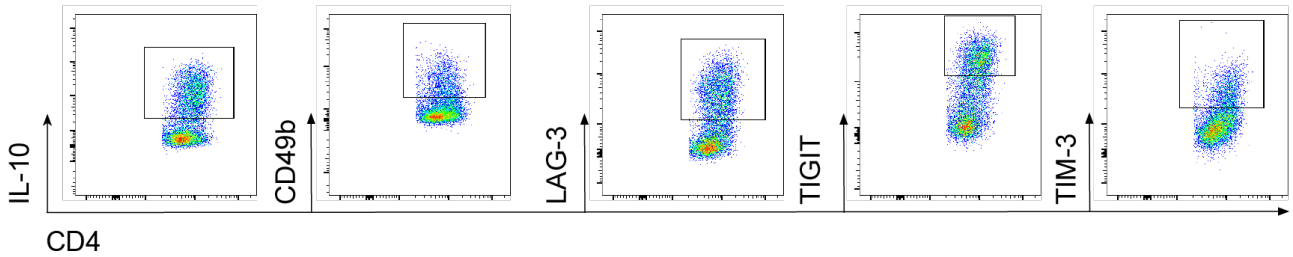

Figure S2: Kidney-derived Foxp3^{neg} IL-10-producing CD4^{+} T cells express CIR

a) Indicates representative dot plots and the gating of stated markers coming from Foxp3^{neg} IL-10 producing CD4^{+} T cells isolated from the kidneys.

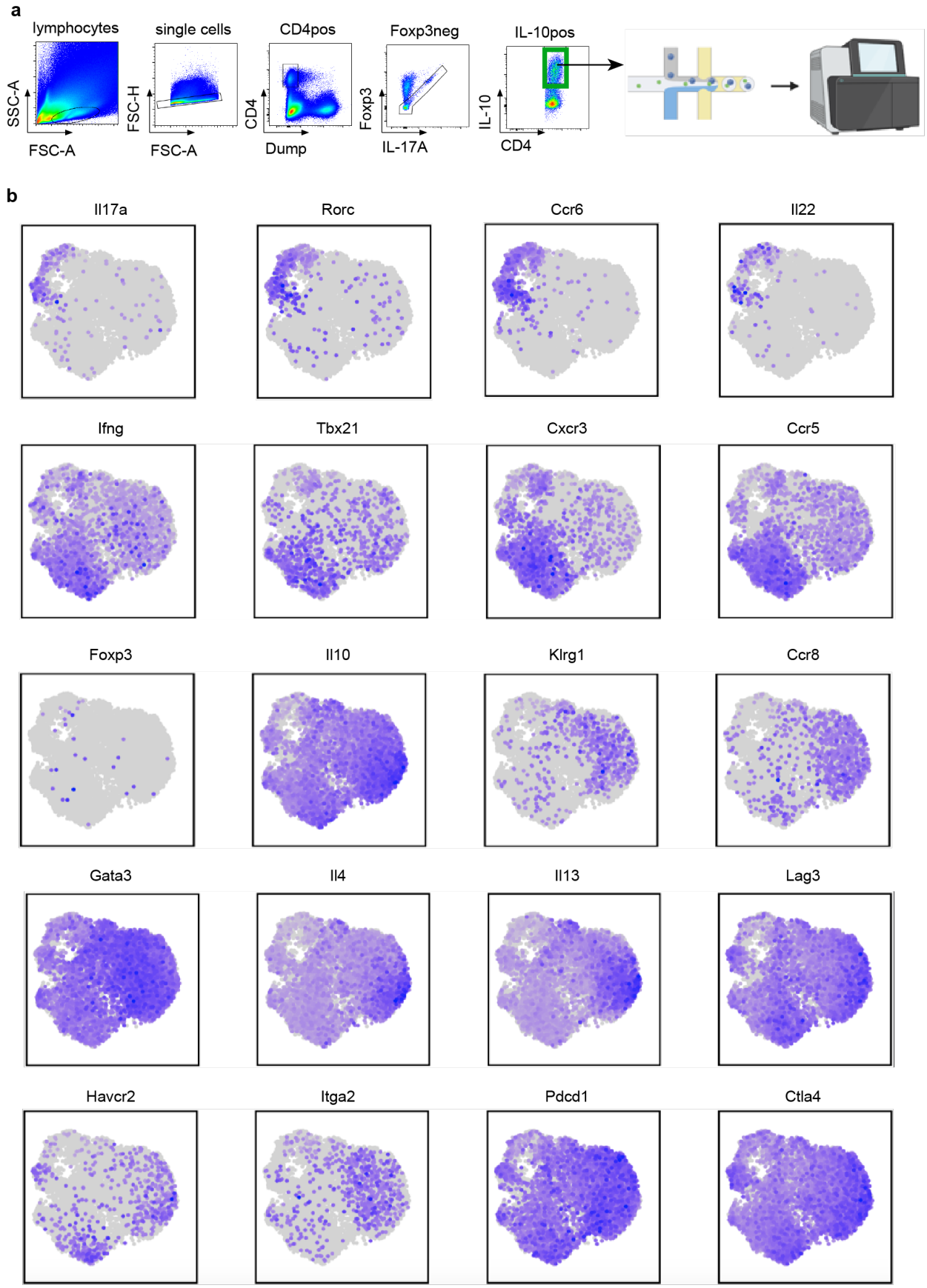

Figure S3: Foxp3^{neg} IL-10-producing CD4^{+} T cells from the kidney show heterogeneous gene expression

a) Indicates dot plots of gating strategy to obtain Foxp3^{neg} IL-10 producing CD4^{+} T cells isolated from the kidneys of control and anti-CD3 mice. **b)** UMAP of gene score of indicated genes in clusters C1-C7 in control group and anti-CD3 treated mice

References

1. Krebs, C.F., et al., *Autoimmune Renal Disease Is Exacerbated by S1P-Receptor-1-Dependent Intestinal Th17 Cell Migration to the Kidney.* Immunity, 2016. **45**(5): p. 1078-1092.
2. Tipping, P.G. and S.R. Holdsworth, *T cells in crescentic glomerulonephritis.* J Am Soc Nephrol, 2006. **17**(5): p. 1253-63.
3. Paust, H.J., et al., *Chemokines play a critical role in the cross-regulation of Th1 and Th17 immune responses in murine crescentic glomerulonephritis.* Kidney Int, 2012. **82**(1): p. 72-83.
4. Steinmetz, O.M., et al., *The Th17-defining transcription factor RORgammat promotes glomerulonephritis.* J Am Soc Nephrol, 2011. **22**(3): p. 472-83.
5. Summers, S.A., et al., *Th1 and Th17 cells induce proliferative glomerulonephritis.* J Am Soc Nephrol, 2009. **20**(12): p. 2518-24.
6. Kluger, M.A., et al., *Stat3 programs Th17-specific regulatory T cells to control GN.* J Am Soc Nephrol, 2014. **25**(6): p. 1291-302.
7. Paust, H.J., et al., *CXCR3+ Regulatory T Cells Control TH1 Responses in Crescentic GN.* J Am Soc Nephrol, 2016. **27**(7): p. 1933-42.
8. Yang, C., et al., *The Regulatory T-cell Transcription Factor Foxp3 Protects against Crescentic Glomerulonephritis.* Sci Rep, 2017. **7**(1): p. 1481.
9. Huber, S., et al., *Th17 cells express interleukin-10 receptor and are controlled by Foxp3(-) and Foxp3+ regulatory CD4+ T cells in an interleukin-10-dependent manner.* Immunity, 2011. **34**(4): p. 554-65.
10. Kluger, M.A., et al., *RORgammat(+)Foxp3(+) Cells are an Independent Bifunctional Regulatory T Cell Lineage and Mediate Crescentic GN.* J Am Soc Nephrol, 2016. **27**(2): p. 454-65.
11. Kluger, M.A., et al., *RORgammat expression in Tregs promotes systemic lupus erythematosus via IL-17 secretion, alteration of Treg phenotype and suppression of Th2 responses.* Clin Exp Immunol, 2017. **188**(1): p. 63-78.
12. Groux, H., et al., *A CD4+ T-cell subset inhibits antigen-specific T-cell responses and prevents colitis.* Nature, 1997. **389**(6652): p. 737-42.
13. Gagliani, N., et al., *Coexpression of CD49b and LAG-3 identifies human and mouse T regulatory type 1 cells.* Nat Med, 2013. **19**(6): p. 739-46.
14. Brockmann, L., et al., *IL-10 Receptor Signaling Is Essential for TR1 Cell Function In Vivo.* J Immunol, 2017. **198**(3): p. 1130-1141.
15. Diefenhardt, P., et al., *IL-10 Receptor Signaling Empowers Regulatory T Cells to Control Th17 Responses and Protect from GN.* J Am Soc Nephrol, 2018. **29**(7): p. 1825-1837.
16. Roncarolo, M.G., et al., *The Biology of T Regulatory Type 1 Cells and Their Therapeutic Application in Immune-Mediated Diseases.* Immunity, 2018. **49**(6): p. 1004-1019.
17. Brockmann, L., et al., *Molecular and functional heterogeneity of IL-10-producing CD4(+) T cells.* Nat Commun, 2018. **9**(1): p. 5457.
18. Chihara, N., et al., *Induction and transcriptional regulation of the co-inhibitory gene module in T cells.* Nature, 2018. **558**(7710): p. 454-459.
19. Gagliani, N., et al., *Th17 cells transdifferentiate into regulatory T cells during resolution of inflammation.* Nature, 2015. **523**(7559): p. 221-5.
20. Krebs, C.F., et al., *Plasticity of Th17 Cells in Autoimmune Kidney Diseases.* J Immunol, 2016. **197**(2): p. 449-57.
21. Hirota, K., et al., *Fate mapping of IL-17-producing T cells in inflammatory responses.* Nat Immunol, 2011. **12**(3): p. 255-63.
22. Kamanaka, M., et al., *Expression of interleukin-10 in intestinal lymphocytes detected by an interleukin-10 reporter knockin tiger mouse.* Immunity, 2006. **25**(6): p. 941-52.
23. Esplugues, E., et al., *Control of TH17 cells occurs in the small intestine.* Nature, 2011. **475**(7357): p. 514-8.
24. Paust, H.-J., et al., *GM-CSF drives immune-mediated glomerular disease by licensing monocyte-derived cells to produce MMP12.* 2022: p. 2022.06.13.495915.
25. Lyons, A.B., S.J. Blake, and K.V. Doherty, *Flow cytometric analysis of cell division by dilution of CFSE and related dyes.* Curr Protoc Cytom, 2013. **Chapter 9**: p. Unit9 11.

26. Pot, C., et al., *Induction of regulatory Tr1 cells and inhibition of T(H)17 cells by IL-27.* Semin Immunol, 2011. **23**(6): p. 438-45.
27. Maynard, C.L., et al., *Regulatory T cells expressing interleukin 10 develop from Foxp3+ and Foxp3- precursor cells in the absence of interleukin 10.* Nat Immunol, 2007. **8**(9): p. 931-41.
28. Collison, L.W. and D.A. Vignali, *In vitro Treg suppression assays.* Methods Mol Biol, 2011. **707**: p. 21-37.
29. Paust, H.J., et al., *Regulatory T cells control the Th1 immune response in murine crescentic glomerulonephritis.* Kidney Int, 2011. **80**(2): p. 154-64.
30. Alikhan, M.A., et al., *Regulatory T cells in renal disease.* Clin Transl Immunology, 2018. **7**(1): p. e1004.
31. Koutrolos, M., et al., *Treg cells mediate recovery from EAE by controlling effector T cell proliferation and motility in the CNS.* Acta Neuropathol Commun, 2014. **2**: p. 163.
32. Desreumaux, P., et al., *Safety and efficacy of antigen-specific regulatory T-cell therapy for patients with refractory Crohn's disease.* Gastroenterology, 2012. **143**(5): p. 1207-1217 e2.
33. Bacchetta, R., et al., *Immunological Outcome in Haploidentical-HSC Transplanted Patients Treated with IL-10-Anergized Donor T Cells.* Front Immunol, 2014. **5**: p. 16.